Iranian Journal of Chemical Engineering
Vol. 16, No. 3 (Summer 2019), IAChE

Reactor Modeling and Kinetic Parameters Estimation for Diethyl Benzene (DEB) Dehydrogenation Reactions

M. E. Zeynali [*]***, H. Abedeni, H. R. Sadri***

Iran Polymer and Petrochemical Institute, Tehran, Iran

ARTICLE INFO

Article history:
Received: 2019-04-09
Accepted: 2019-10-01

Keywords:
Diethyl Benzene,
Dehydrogenation,
Reactor Modeling,
Divinyl Benzene

ABSTRACT

Divinyl benzene (DVB) is produced by the catalytic dehydrogenation of DEB at high temperatures and atmospheric pressure. Ethylvinyl benzene (EVB) was produced as a useful chemical during the dehydrogenation of DEB. Moreover, some other liquid and gaseous by-products were produced during dehydrogenation. A setup was developed to conduct experiments concerning the DEB dehydrogenation reactions to prepare DVB in different conditions. Model equations for DEB dehydrogenation reactor were solved by genetic algorithm (GA) method using MATLAB software. Reaction rate constants and absorption coefficients were determined at various temperatures. The conversion of DEB and ethyl vinyl benzene (EVB) in the reactor was predicted by mathematical modeling and compared with experimental results. The comparison showed good agreement between experimental and modeling results. The combined effects of DEB flow rate and catalyst weight as a time factor were investigated on the conversion of DEB and production of EVB and DVB. The effects of temperature on the consumption of DEB and production of EVB and DVB in the tubular reactor were investigated.

1. Introduction

DVB is an extremely versatile cross-linking agent that improves polymer properties. Since the dehydrogenation reaction is endothermic and volume-increasing, a large amount of superheated steam (volume ratio of H2O/DEB=10) is used to supply heat, lower the partial pressure of the reactants to shift the equilibrium to DVB production, and avoid the formation of carbonaceous deposits to preserve the catalyst activity. However, much of the latent heat of steam is lost at the gas–liquid separator instead of being reclaimed, similar to the dehydrogenation of ethyl benzene [1].

DVB is produced by the catalytic dehydrogenation of DEB at high temperatures and below atmospheric pressure. The catalyst is based on iron oxide and chromium oxides and some other metallic oxides. EVB is produced during the production of DVB. Some other liquids and gaseous materials are produced during the process. Various parameters affect the preparation of DVB [2-3]. The most important parameters are temperature, weight of catalyst, steam flow

[*]Corresponding author: m.zeynali@ippi.ac.ir

rate, catalyst type, catalyst pellet dimensions, pore size and pore size distribution of catalyst, and inert gas flow rate. The reaction is equilibrium limited and endothermic. There are some papers in the literature on the dehydrogenation of diethyl benzene [4-5]; however, little information about its kinetics remains for use.

A kinetic study of diethyl benzene dehydrogenation was performed by Forni and Valerio [6]. Kinetic parameters used for the dehydrogenation process of ethyl benzene to styrene were determined using the catalyst deactivation function based on the reactant conversion model by Atanda and Al- Yassir [7]. Some of the important elements of the theory and of the practical applications of the kinetics of heterogeneous catalytic reactions were given by Petrov et al. [8]. Various techniques were introduced to determine the kinetic parameters in heterogeneous catalytic reactions [9-13]. From a fundamental point of view, kinetics contributes to a better understanding of reaction mechanisms and of the effect of a catalyst upon them. From a more practical point of view, accurate kinetic equations are of crucial importance in the reliable design or simulation of reactors [14]. To optimize non-steady state processes such as periodic reactant feed or reverse flow time-dependent surface processes such as the formation and consumption of active sites and adsorbed intermediates, they must be described first [15-16]. An experimental tool for performing transient experiments is the temporal analysis of the products (TAP) [17]. Analytical and numerical methods are employed for estimating the kinetic parameters. The estimation of kinetic parameters based on the analytical solution is fast; however, to investigate more complex reactions, a method based on a complete numerical solution is required. The kinetic parameters can be estimated by nonlinear and linear regression analyses. A method was presented by Xu and Hoffmann [18] to transform the nonlinear regression problem through the kinetic study of complex heterogeneous catalytic reactions into a linear regression problem. Scaling up and modeling of Cr(VI) removal using nano iron-based coated biomass as packing material in the fixed-bed reactor has been reported in the literature [19]. The dynamic one-dimensional pseudo-homogeneous model for Fischer-Tropsch fixed-bed reactors was studied by Mendez et al. [20]. The CFD model of coal pyrolysis in the fixed bed reactor was also reported [21].

Nowadays, the mathematical modeling and prediction of process behavior play an important role in process development and achievement and have received significant consideration from researchers. Considering the various uses of DVB in research and industry, modeling and reactor design is a requirement for process development. Since there are a few papers in the open literature, the present study has made an attempt to investigate the process behavior of DVB production experimentally and by mathematical modeling.

The main DEB dehydrogenation reactions are as follows:

$$\mathrm{DEB} \underset{}{\overset{-H_2}{\rightleftharpoons}} \mathrm{EVB} \overset{-H_2}{\rightleftharpoons} \mathrm{DVB}$$

2. Experimental

2.1. Materials and methods

The equipment and devices, which were used in the experiments, include 1-quartz tubular reactor, 2-furnace, 3-flowmeters, 4-syringe pumps, 5-pre heaters, 6-thermocouples, and 7-condenser. The heating zone of the furnace was 30 cm. Nitrogen gas was used as the

carrier of the DEB and steam. The flow rate of nitrogen was adjusted to 20 cc/min for all experiments. Experimental grade DEB was used in the experiments and purchased from Sigma-Aldrich. Liquid water and DEB were fed by two syringe pumps into the evaporator at adjusted flow rates. The ratio of water to DEB flow rate was adjusted to 5/1 for all experiments. DEB and water should be preheated before being fed to the reactor. This was performed by two preheaters. Before conducting the experiments, the calibration of syringe pumps and the accuracy of flow rates were ensured. The fixed bed tubular reactor was loaded with catalyst pellets. The loaded reactor was kept for 24 h at 600 ºC to activate the catalyst to run the experiments. Quartz beads were used in front of the catalyst pellets bed to ensure uniform heat transfer and flow to prevent channeling of the gaseous reactant and hot spot formation in the reactor. At the end of the reactor, a quartz condenser was used to condense the products. The liquid products were collected by a balloon at the bottom of the condenser. The collected liquid had two phases: hydrocarbon phase and aqueous phase. Two phases were separated by a decanter and hydrocarbon phase was sent for analysis by GC-mass. Then, 10, 20, 30, and 40 gr catalysts were used in the experiments. Temperatures 550, 560, 570, 580, 590, and 600 ºC were used for the experiments. By keeping the water to DEB flow rate ratio constant, the flow rate of DEB varied from 5 cc/h with 1 cc/h increment to 10 cc/h in a typical GC-mass spectrum, and chemical analysis of the products is shown in Figure 1 and Table 1 respectively.

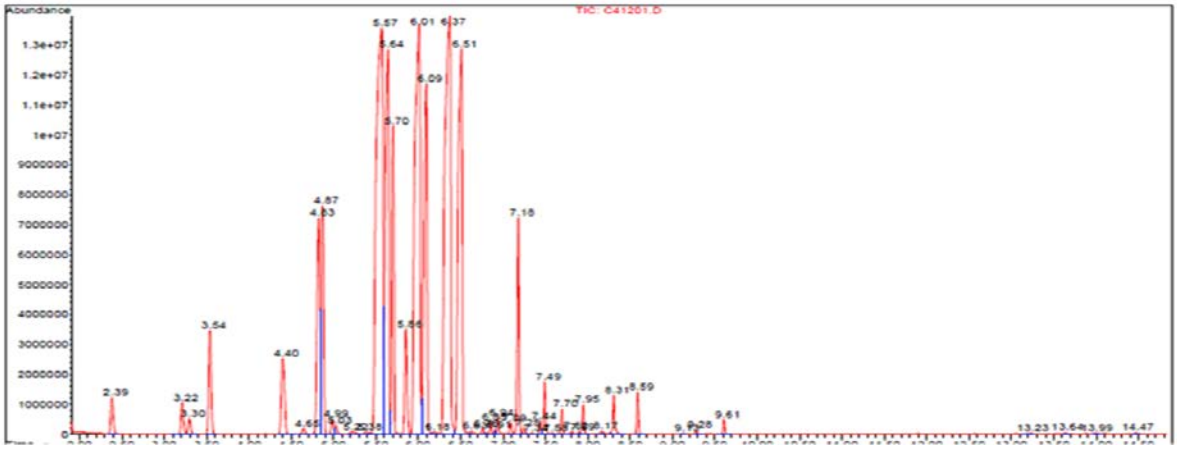

Figure 1. GC-mass spectrum for the sample prepared at 600 ºC with 40 g catalyst.

Table 1

GC-mass analysis results of liquid products at 600 ºC with 40 g catalyst.

Substance	Weight %
DEB	15.22
EVB	26.4
DVB	47.88
Styrene	0.6
1-Ethyl 3- Methyl Benzene	0.91
1-Ethenyl 3-Ethyl Benzene	3.1
1-ethenyl 4-Methyl Benzene	2.95
2-Methyl 1-Propen Benzene	0.36
Naphthalene	2.58

2.2. Model equations

Any attempt to formulate the rate equation of heterogeneous reactions follows the basic laws of chemical kinetic, which is seen in homogeneous reactions. However, it should be considered that these laws are employed when the concentration and temperature of the reaction on the surface of the catalyst are used in reaction rate determination. Considering the absorption characteristic of the system, these locations are not necessarily required to be on or over the active sites. To develop a kinetic model, reaction rate constants and the extent of absorption should be linked to the concentration of fluid components in contact with the surface of the catalyst.

Langmuir-Hinshelwood model is used for the kinetics of heterogeneous catalytic reactions, which can be shown by a simple mechanism. In the Langmuir-Hinshelwood mechanism, the catalyst surface is modeled assuming energy is the same around the surface and there is not any energetic interaction between absorbed components on the surface. These are assumptions that Langmuir made to obtain various terms in the surface absorption model. Each reactant is absorbed at surface sites. Then, it is assumed that the reaction of absorbed molecules takes place on the surface and the products are formed on the surface, as well. In continuation, products are desorbed from the surface. Often, it is assumed that the surface reaction is irreversible; however, absorption and desorption processes are reversible.

Reaction rate equations based on the Forni for dehydrogenation of DEB are as follows [6]:

$$r_1 = \frac{k_1 b_D (P_D - \frac{P_E P_H}{K_1})}{(1 + b_D P_D + b_E P_E + b_V P_V + b_H P_H + b_A P_A)^2} \quad DEB \rightleftharpoons EVB + H_2 \qquad (1)$$

$$r_2 = \frac{k_2 b_E (P_E - \frac{P_V P_H}{K_2})}{(1 + b_D P_D + b_E P_E + b_V P_V + b_H P_H)^2} \quad EVB \rightleftharpoons DVB + H_2 \qquad (2)$$

where P_i is the partial pressure, b_i is the absorption coefficient, and D, E, V, and H stand for P-DEB, p-EVB, p-DVB, and hydrogen, respectively. K_1 and K_2 are gas phase equilibrium constants, and k_1 and k_2 are reaction rate constants.

The rate equations are:

$$\begin{aligned} -\frac{dx_D}{d\tau} &= r_{DE} + r_{DL} - r_{ED} \\ \frac{dx_E}{d\tau} &= r_{DE} - r_{EV} - r_{ED} + r_{VE} - r_{EL} \\ \frac{dx_V}{d\tau} &= r_{EV} - r_{VE} - r_{VL} \\ \frac{dx_L}{d\tau} &= r_{DL} + r_{EL} + r_{VL} - r_{VL} \end{aligned} \qquad (3)$$

where x_i is the molar fraction and represents the fed hydrocarbon of the substance i, r_{ij} is the rate of transformation of the i^{th} substance in the j^{th} one; τ=W/F is the time factor, W is

the catalyst weight (g), F is the DEB flow rate (mol/h); the subscript L is the light hydrocarbon due to cracking side reactions. Light hydrocarbons in EVB and DVB production and EVB consumption reactions are small quantities and ignored; therefore, only DEB dehydrogenation reaction is considered here:

$$-\frac{dx_D}{d\tau}=\frac{\mathrm{k_1 b_D}\left(\mathrm{P_D}-\frac{\mathrm{P_E P_H}}{\mathrm{K_1}}\right)}{(1+b_D P_D+\mathrm{b_E P_E}+\mathrm{b_V P_V}+\mathrm{b_H P_H})^2}+k_3 P_D$$

$$\frac{dx_E}{d\tau}=\frac{\mathrm{k_1 b_D}\left(\mathrm{P_D}-\frac{\mathrm{P_E P_H}}{\mathrm{K_1}}\right)-\mathrm{k_2 b_E}(\mathrm{P_E}-\frac{\mathrm{P_V P_H}}{\mathrm{K_2}})}{(1+b_D P_D+\mathrm{b_E P_E}+\mathrm{b_V P_V}+\mathrm{b_H P_H})^2} \quad (4)$$

$$\frac{dx_V}{d\tau}=\frac{\mathrm{k_2 b_E}(\mathrm{P_E}-\frac{\mathrm{P_V P_H}}{\mathrm{K_2}})}{(1+b_D P_D+\mathrm{b_E P_E}+\mathrm{b_V P_V}+\mathrm{b_H P_H})^2}$$

$$\frac{dx_L}{d\tau}=k_3 P_D$$

where k_3 is the reaction rate constant of the light hydrocarbons.

For simplification, the following terms are defined:

w= (mole fraction of DEB);
y= (mole fraction of EVB);
z= (mole fraction of DVB);
a= (mole fraction of water)

The total pressure is assumed to be equal to 1 atm. According to Raoult's law, we have:

$y_i=p_i$

According to the above definitions, the equations are simplified as:

$$-\frac{dw}{d\tau}=\frac{\mathrm{k_1 b_D}\left(\mathrm{w}-\frac{\mathrm{y}}{\mathrm{K_1}\sum}(y+2z)\right)}{(\sum+b_D w+\mathrm{b_a y}+\mathrm{b_b z})^2}+k_3\frac{w}{\sum}$$

$$\frac{dy}{d\tau}=\frac{\mathrm{k_1 b_D}\left(\mathrm{w}-\frac{\mathrm{y}}{\mathrm{K_1}\sum}(y+2z)\right)-\mathrm{k_2 b_E}\left(\mathrm{y}-\frac{\mathrm{z}}{\mathrm{K_2}\sum}(y+2z)\right)}{(\sum+b_D w+\mathrm{b_a y}+\mathrm{b_b z})^2} \quad (5)$$

$$\frac{dz}{d\tau}=\frac{\mathrm{k_2 b_E}\left(\mathrm{y}-\frac{\mathrm{z}}{\mathrm{K_2}\sum}(y+2z)\right)}{(\sum+b_D w+\mathrm{b_a y}+\mathrm{b_b z})^2}$$

$$\frac{dx}{d\tau}=k_3\frac{w}{\sum}$$

where $\sum$= 1 + a + 2 y + z; $b_a = b_E + b_H$; $b_b = b_V + 2\ b_H$.

3. Results and discussion

The given reaction rate equations were simulated by MATLAB. In comparison with C^{++} and Fortran, MATLAB needs a short programming time. It is efficient software with high capabilities regarding programming and computation. In our simulation, Genetic

Algorithm (GA) has been used frequently. GA is a family of computational models inspired by nature. These algorithms encode a potential solution to a specific problem on a simple chromosome like data structure and apply recombination operators to these structures so as to preserve critical information. GAs are often viewed as function optimizers, although the range of problems to which GAs have been applied is quite broad. The implementation of GA begins with a population of (typically random) chromosomes. One then evaluates these structures and allocates reproductive opportunities in such a way that those chromosomes that represent a better solution to the target problem are given more chances to "reproduce" than those chromosomes which are poorer solutions. The goodness of a solution is typically defined with respect to the current population.

Now, the modeling of experimental results is done here. To do so, the target function, defined earlier, was used. The computer program was written in such a way that, in each cycle, the temperature of the experimental results to be modeled was used. To run the program, an initial condition is required. Considering that the experimental results at 600 ºC are higher than other temperatures, this temperature has been used as the reference value at other temperatures. For the initial conditions, the data provided by Forni [6] obtained by genetic algorithm was used at 600 ºC. The modeling results are presented in Figs. 2-6.

After running the program at 600 ºC, the results were used as initial values at other temperatures. The data for other temperatures do not exist in abundance than the data for 600 ºC; therefore, to increase the accuracy of the results, the upper and lower limits were confined. The constants were shown to have a direct relationship with temperature; therefore, the upper limit was multiplied by 0.98 and the lower limit was multiplied by 0.7. In addition, considering the error at other temperatures, various lower limits were used to increase the accuracy.

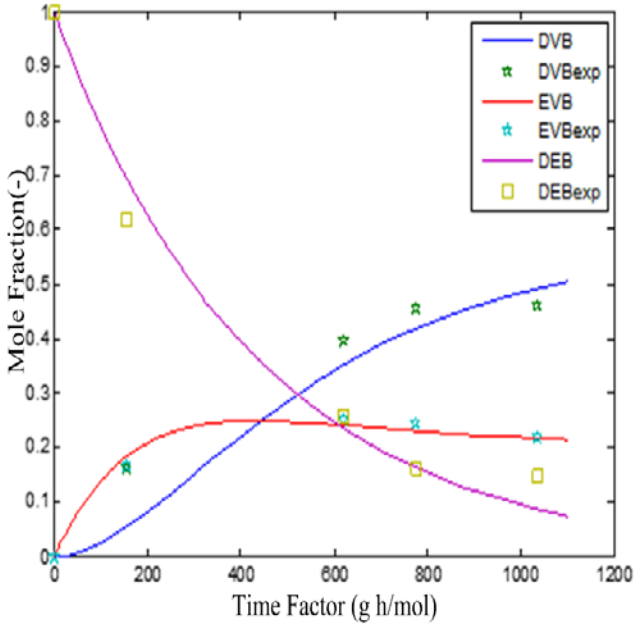

Figure 2. Experimental and modeling results of mole fraction vs. time for DVB and EVB at 600 ºC.

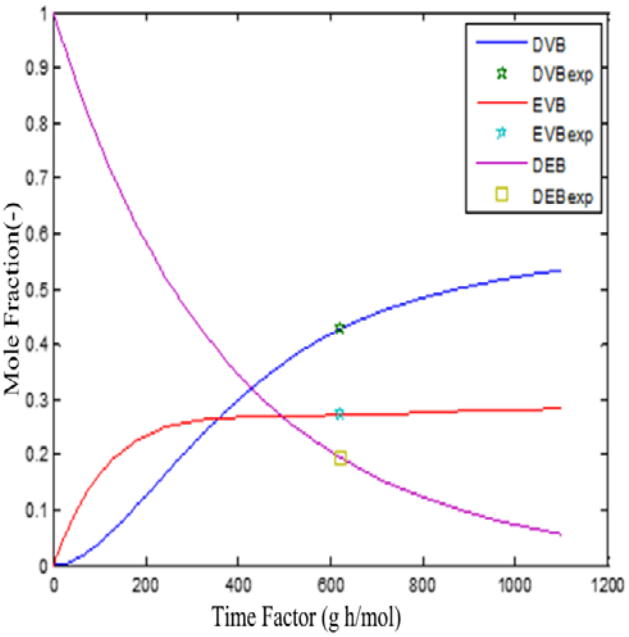

Figure 3. Experimental and modeling results of mole fraction vs. time for DVB and EVB at 590 ºC.

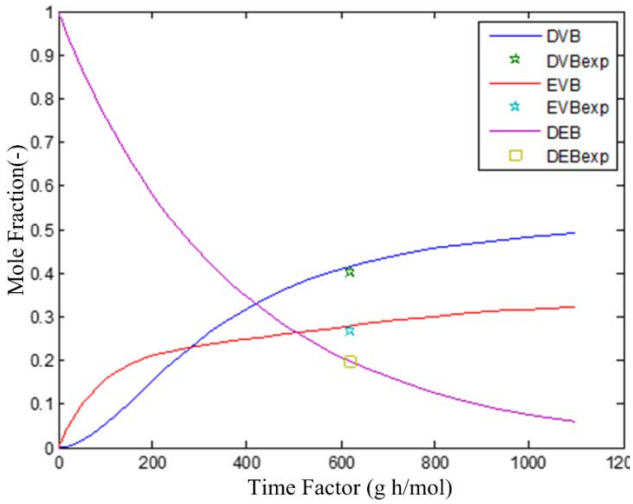

Figure 4. Experimental and modeling results of mole fraction vs. time for DVB and EVB at 580 ºC.

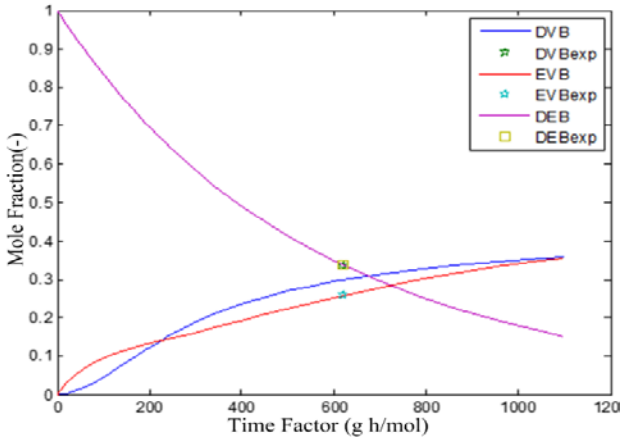

Figure 5. Experimental and modeling results of mole fraction vs. time for DVB and EVB at 570 ºC.

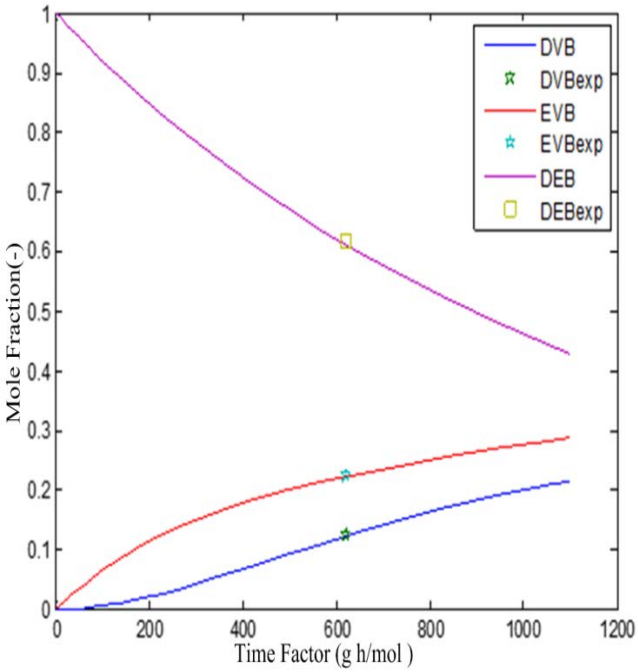

Figure 6. Experimental and modeling results of mole fraction vs. time for DVB and EVB at 550 ºC.

The logarithm of reaction rate constants versus the inverse of temperature is plotted. The results of reaction rate constants are shown in Figs. 7-13.

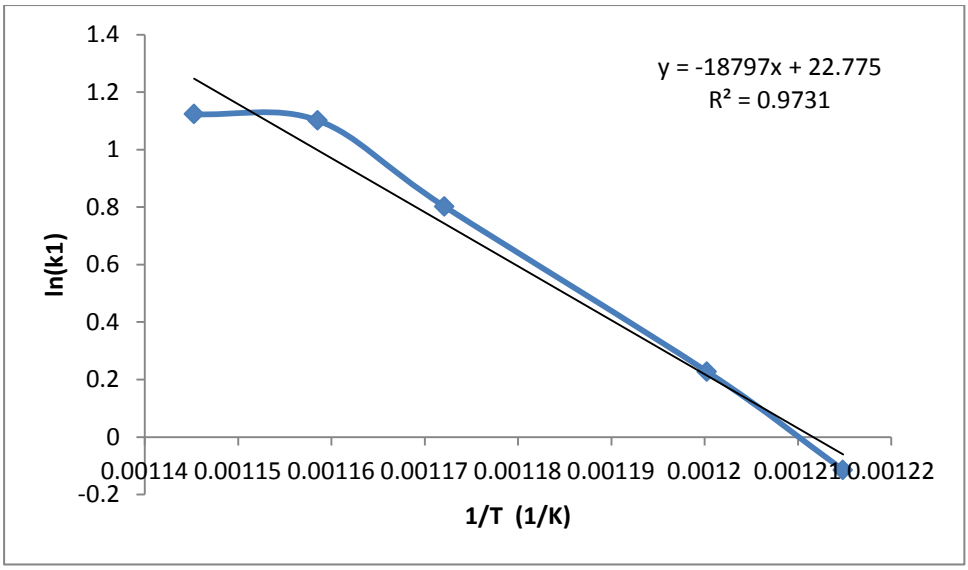

Figure 7. $\ln(k_1)$ vs. inverse of temperature (K).

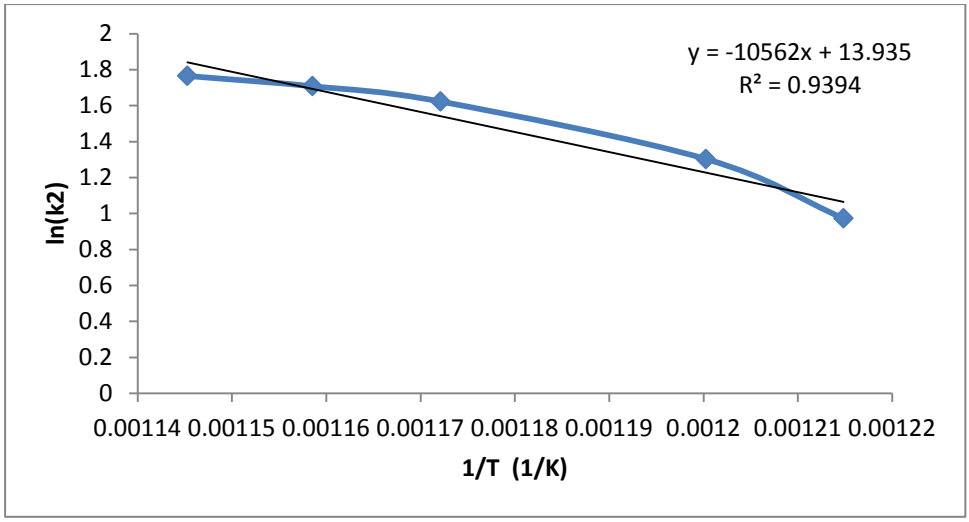

Figure 8. ln(k_2) vs. inverse of the temperature (K).

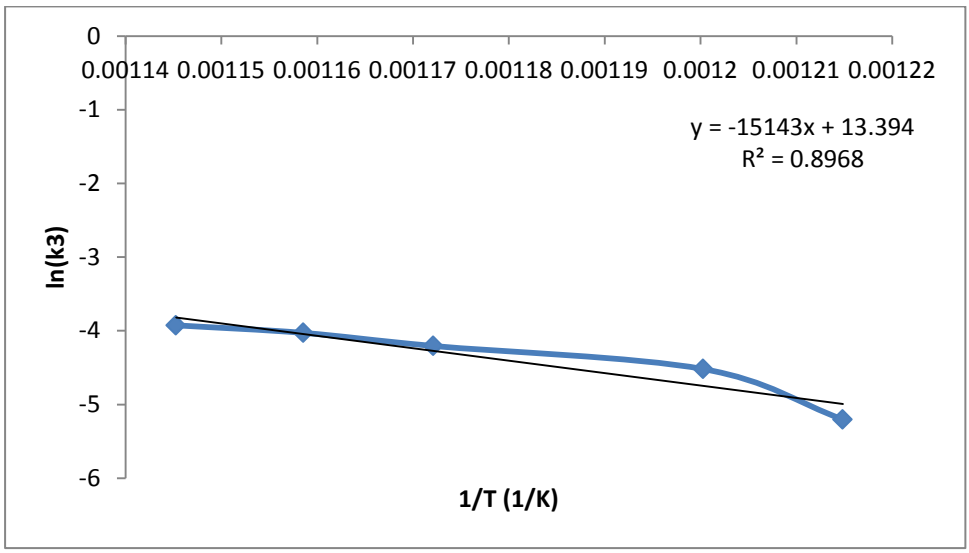

Figure 9. ln(k_3) vs. inverse of the temperature (K).

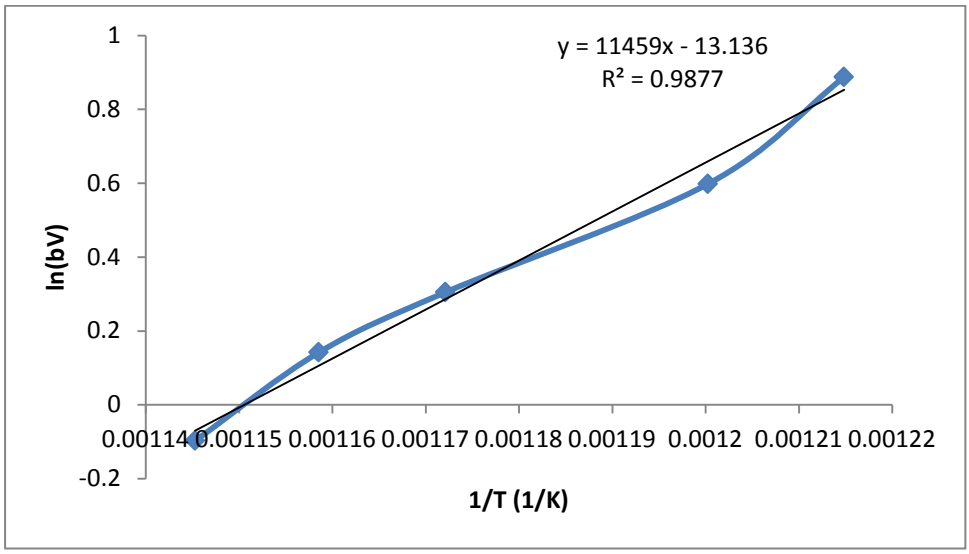

Figure 10. ln(b_v) vs. inverse of the temperature (K).

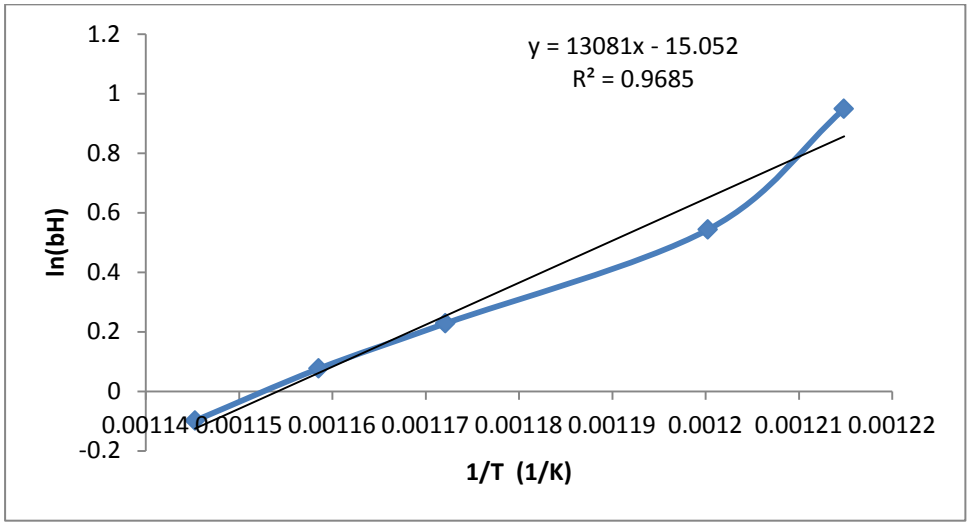

Figure 11. ln(b_H) vs. inverse of the temperature (K).

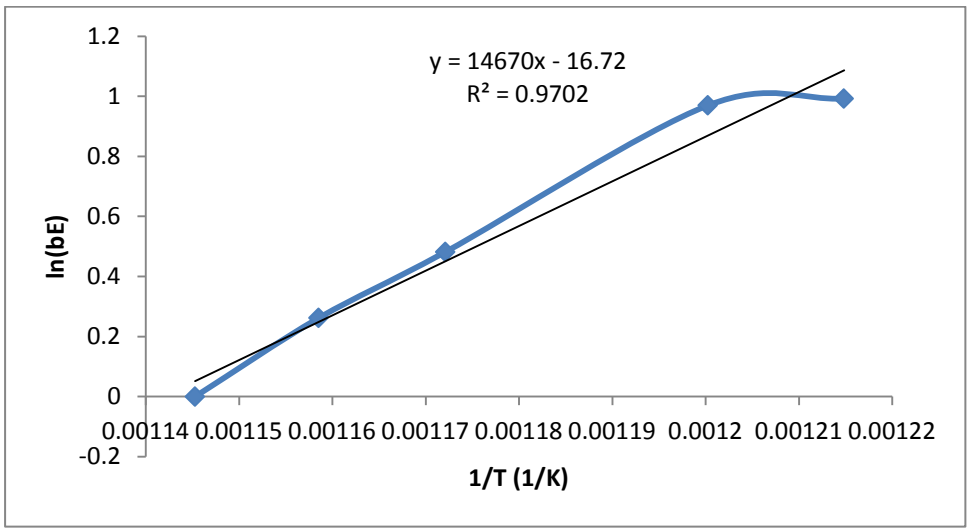

Figure 12. ln(b_E) vs. inverse of the temperature (K).

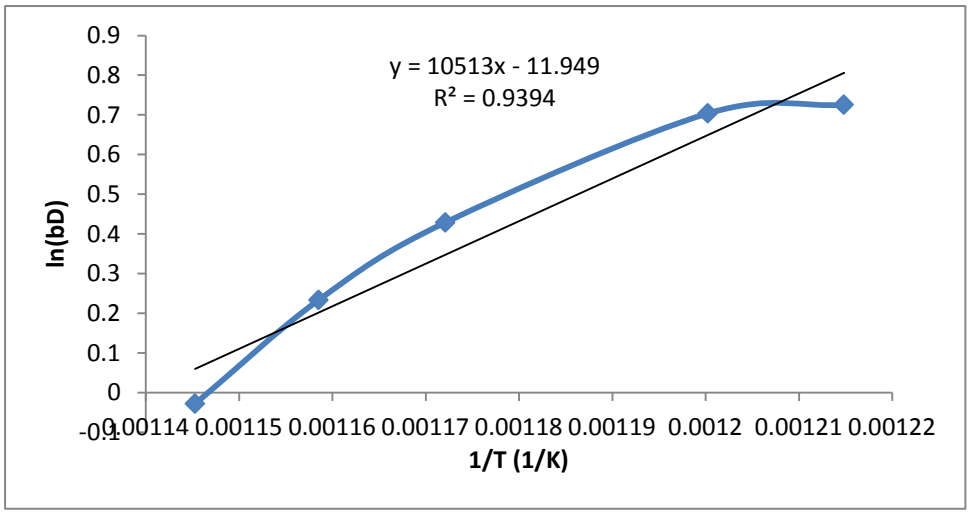

Figure 13. ln(b_D) vs. inverse of the temperature (K).

It is observed that accuracy has been reduced compared with Forni´s experimental results. The error can result from the increased number of points and partly from the fitting of the model with the experimental data. Based on the accuracy of the measurement devices, there could be some errors in experimental data, too. Now, the initial conditions for target function have been obtained.

The reaction rate constants are known, and the consumption rate of DEB and production rate of DVB and EVB can be obtained as shown in Figures 14-15. These results were obtained through the simultaneous solving of equations using ODE23b solver with MATLAB software.

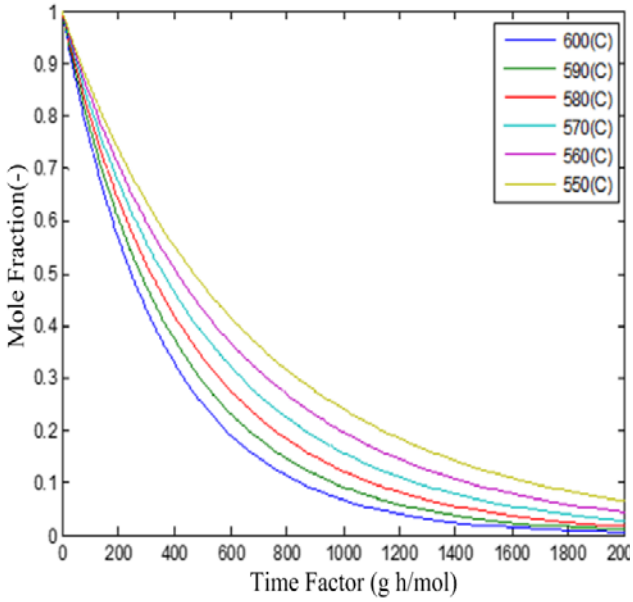

Figure 14. DEB consumption at various temperature.

The results of DEB consumption are presented in Figure 14. As seen, by increasing the time factor, the conversion of DEB increases and the mole fraction of DEB reduces. With an increase in temperature, the reaction rate constants increase, meaning that the detachment of hydrogen from DEB is easier at high temperatures. Therefore, the curves at a constant time factor and at lower temperatures shown in Figure 14 shift to lower conversions.

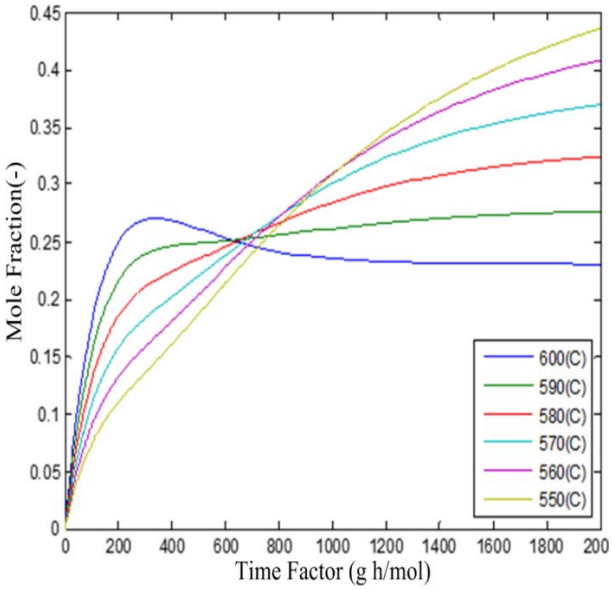

Figure 15. EVB production at various temperatures.

The production rate of EVB at various temperatures is presented in Figure 15. The production rate of EVB is different from the production rate of DVB. The difference is due to the fact that EVB is an intermediate material. It is produced by the dehydrogenation of DEB and is consumed by the production of DVB. At temperatures ranging from 550 ºC to 580 ºC with an increase in the time factor, the production rate of EVB increases. This trend shows that in competition between EVB and DVB, the production of EVB wins. However, at temperatures between 590 ºC and 600 ºC, the curve of EVB has a maximum. This shows that, at these temperatures, initially, the detachment of hydrogen from DEB is more than that from EVB; however, given the increasing time factor, the detachment of hydrogen from EVB is seen greatly. According to Figure 15, the curves cross each other around a point in the graph.

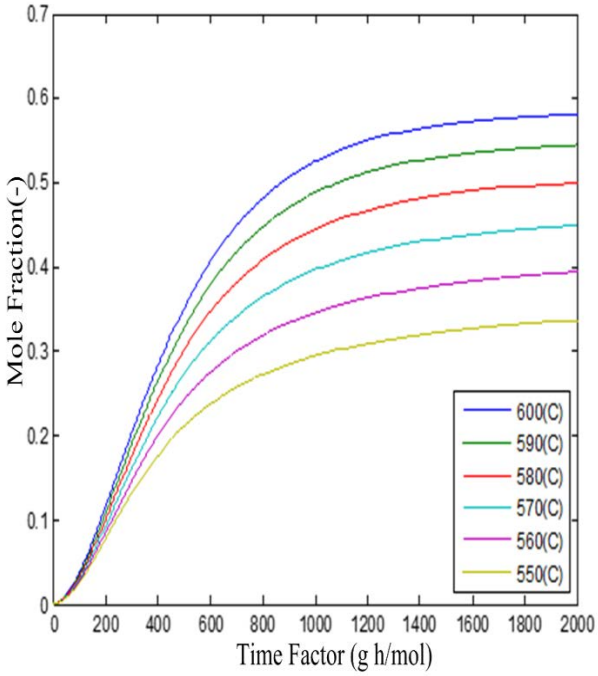

Figure 16. DVB production at various temperatures.

Figure 16 presents the production rate of DVB. The aim is to obtain maximum conversion or mole fraction of DVB. As observed earlier, the mole fraction of DVB increases and, then, stays almost constant. The initial ascending trend of DVB mole fraction shows the conversion of EVB to DVB. According to Figures 15 and 14, it is observed that the consumption of DEB and production of EVB reach constant values at the time factor above 800 (gr h/mol). This causes the production of DVB to remain almost constant at the time factor above 800 (gr h/mol). Moreover, it is observed that with an increase in temperature, the curves shift upward and production of DVB increases.

Figures 17-18 demonstrate the model prediction and experimental results for the consumption of DEB.

Figures 19 and 20 demonstrate the model prediction and experimental results for the production of EVB.

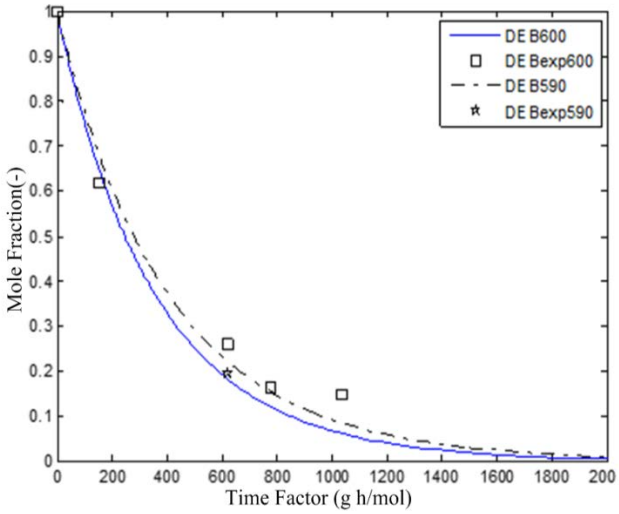

Figure 17. DEB consumption at 590 ºC and 600 ºC in comparison with experimental results.

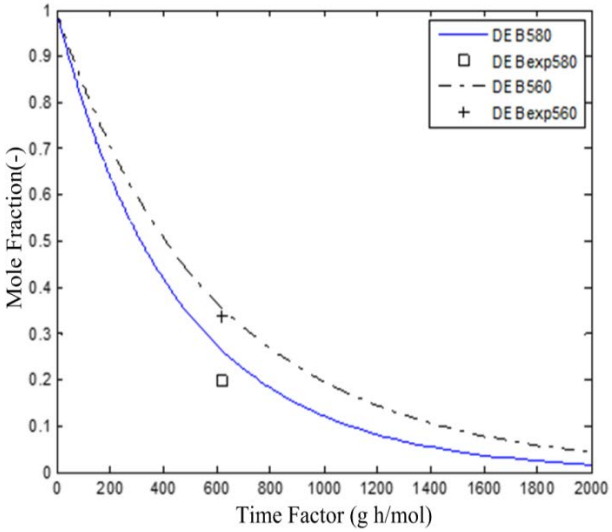

Figure 18. DEB consumption at 560 ºC and 580 ºC in comparison with experimental results.

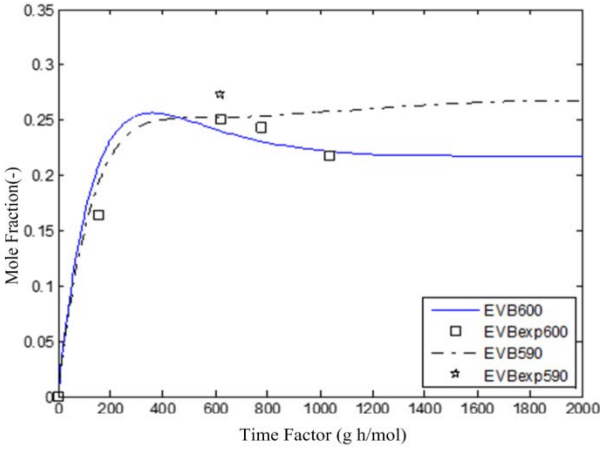

Figure 19. EVB production at 590 ºC and 600 ºC in comparison with experimental results.

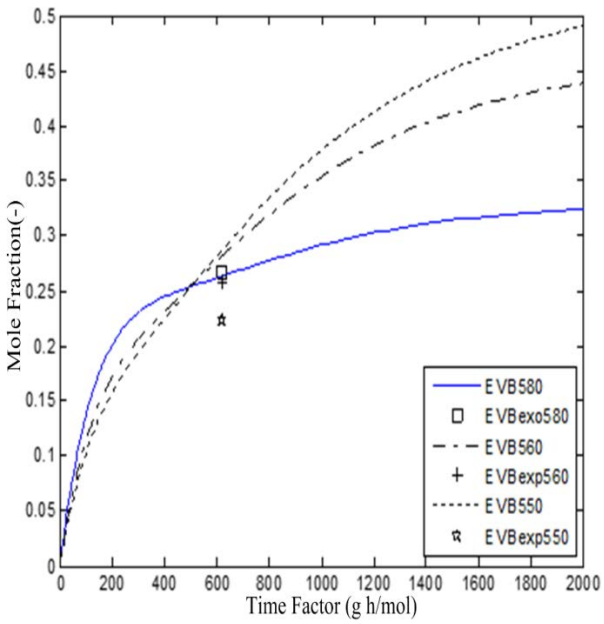

Figure 20. EVB production at 550 ºC, 560 ºC, and 580 ºC in comparison with experimental results.

Figures 21 and 22 demonstrate the model prediction and experimental results of the production of DVB.

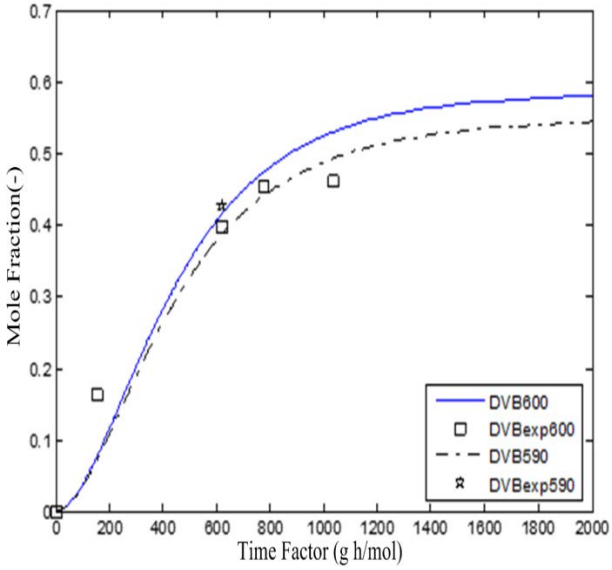

Figure 21. DVB production at 590 ºC and 600 ºC in comparison with experimental results.

The best values of reaction rate constants were determined by minimizing the error. As mentioned before, the important aim of mathematical modeling is to predict the production of DVB at various catalyst weights. For this reason, the mole fraction of DVB was plotted versus catalyst weight at various temperatures in Figure 23. Increasing catalyst weight and decreasing the DEB flow rate exerted the same effect on reactor performance. These two parameters affect the residence time of feed in the reactor.

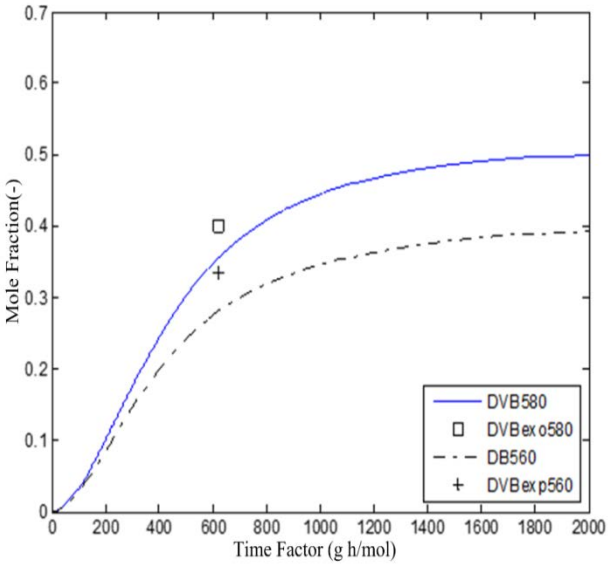

Figure 22. DVB production at 560 ºC and 580 ºC in comparison with experimental results.

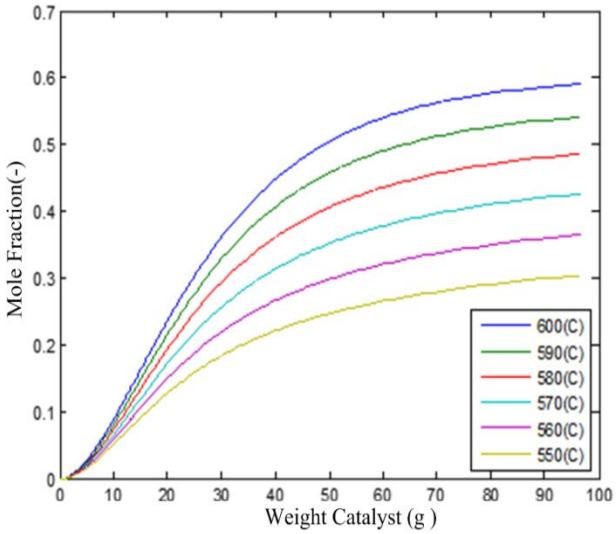

Figure 23. DVB production vs. catalyst weight at various temperatures.

Figure 23 shows that with an increase in temperature, the mole fraction of DVB

increases at a constant catalyst weight. This result results from an increase in reaction rate constants with an increase in temperature. Moreover, it is observed that, at a constant temperature, an increase in catalyst weight causes an increase in the mole fraction of DVB. Initially, the slope of the curve or the intensity of the increase in DVB mole fraction is high. For the catalyst above 40 g, the slope drops and mole fraction of DVB almost remains constant and reaches an almost plateau section. For example, at 600 ^{o}C with 40 g catalyst, the mole fraction of DVB is 0.47 and is 0.56 with 80 g catalyst. In other words, by doubling the catalyst weight, the fraction increases only by 0.09. As implied, it is not economically feasible to increase the catalyst weight above 40 g by keeping other parameters constant.

4. Conclusions

DEB dehydrogenation reactions to prepare DVB and EVB were conducted. The effects of time factor (an important parameter in reactor design) on DEB conversion were obtained. DVB production versus catalyst weight (as a sensible factor) at various temperatures was determined. It is observed that, by increasing the time factor, the conversion of DEB increases and the mole fraction of DEB reduces in the reactor effluent. Since the dehydrogenation reaction is endothermic with the increasing temperature, the consumption of DEB and the production of EVB and DVB increase. The reaction is equilibrium limited and the highest conversion of DEB is achieved at 600 ^{o}C; above this temperature, the thermal cracking occurs. The results show that it is not economically feasible to increase the catalyst weight above 40 g by keeping other parameters constant.

Acknowledgements

The authors appreciate Iran Polymer and Petrochemical Institute for financial support to carry out this research.

References

[1] Matsui, J. T. and Sodesawa, F., "Influence of carbon dioxide addition upon decay of activity of a potassium promoted iron oxide catalyst for dehydrogenation of ethylbenzene", *Appl. Catal. A*, **67**, 179 (1991).

[2] Zeynali, M. E., "Effects of different processing parameters on divinylbenzene (DVB) production rate", *Chem. Sci. J.*, **CSJ22**, 1 (2011).

[3] Chen, S., Sun, A., Qin, Z. and Wang, J., "Reaction coupling of diethylbenzene dehydrogenation with water-gas shift over alumina-supported iron oxide catalysts", *Catal. Commun.*, **4**, 441 (2003).

[4] Rao, K. N., Reddy, B. M. and Park, S. E., "Novel CeO_2 promoted TiO_2-ZrO_2 nano-oxide catalysts for oxidative dehydrogenation of p-diethylbenzene utilizing CO_2 as soft oxidant", *Appl. Catal. B*, **100** (3-4), 472 (2010).

[5] Kamiguchi, S., Kondo, K., Kodoman, M. and Chihara T., "Catalytic ring attachment isomerization and dealkylation of diethylbenzene over halide clusters of group 5 and group 6 transition metals", *J. Catal*, **223** (1), 54 (2004).

[6] Forni, L. and Valerio, A., "Kinetics of diethylbenzene catalytic dehydrogenation", *Ind. Eng. Chem. Process Des. Develop*, **10** (4), 552 (1971).

[7] Atanda, L. and Al-Yassir, N., "Kinetic modeling of ethylbenzene

dehydrogenation over hydrotalcite catalysts", *Chem. Eng. J.*, **171** (3), 1387 (2011).

[8] Petrov, L. A., Alhamed, Y., Al-Zahrani, A. and Daous, M., "Role of chemical kinetics in the heterogeneous catalysis studies", *Chin. J. Catal.*, **32** (6-8), 1085 (2011).

[9] Cruz, S. C., Rothenberg, G., Westerhuis, J. A. and Smilde, A. K., "Estimating kinetic parameters of complex reactions using a curve resolution based method", *Chemom. Intell. Lab. Syst*, **91**, 101 (2008).

[10] Kaufman, D., Sterner, C., Masek, B., Svenningsen, R. and Samuelson, G., "An NMR kinetics experiment", *J. Chem. Educ.*, **59**, 885 (1982).

[11] Bisby, R.H. and Thomas, E.W., "Kinetic analysis by the method of nonlinear least squares: A reaction involving consecutive steps", *J. Chem. Educ*., **63**, 990 (1986).

[12] Chrastil, J., "Determination of first-order consecutive reversible reaction kinetics", *Comput. Chem*., **17**, 103 (1993).

[13] Bijlsma, S. and Smilde, A. K., "Application of curve resolution based method to kinetic data", *Anal. Chem. Acta*, **396**, 231 (1999).

[14] Froment, G. F., "The kinetics of complex catalytic reactions", *Chem. Eng. Sci.*, **42** (5), 1073 (1987).

[15] Weismantel, L., Stockel, J. and Eming, G., "Improvement of selectivity with two-step process for the oxidation of isobutyric acid", *Appl. Catal. A*, **137**, 129 (1996).

[16] Golbig, K. G. and Werther, J., "Selective synthesis of maleic anhydride by spatial separation of n-butane oxidation and catalyst reoxidation", *Chem. Eng. Sci*., **52**, 583 (1997).

[17] Soick, M., Wolf, D. and Baerns, M., "Determination of kinetic parameters for complex heterogeneous catalytic reactions by numerical evaluation of TAP", *Chem. Eng. Sci*., **55**, 2875 (2000).

[18] Xu, J. and Haffmann, U., "Some strategies for the kinetic study of complex heterogeneous catalytic reactions", *Chem. Eng. Technol*., **13**, 397 (1990).

[19] Vilardi, G., Rodriguez, J., Miguel, J., Pulido, O., Palma, L. and Vedone, N., "Fixed-bed reactor scale-up and modelling for Cr(VI) removal using nano iron-based coated biomass as packing material", *Chemical Engineering Journal*, **361**, 990 (2019).

[20] Mendez, C. I. and Ancheyta, J., "Dynamic one-dimensional pseudohomogeneous model for Fischer-Tropsch fixed-bed reactors", *Fuel*, **252**, 371 (2019).

[21] Oian, Y., Zhan, J., Yu, Y., Xu, G. and Liu, X., "CFD model of coal pyrolysis in fixed bed reactor", *Chem. Eng. Sci*, **200**, 1 (2019).